JOURNAL OF
ENVIRONMENTAL HYDROLOGY
The Electronic Journal of the International Association for Environmental Hydrology
On the World Wide Web at http://www.hydroweb.com
VOLUME 15 2007

MATHEMATICAL MODELS FOR ESTIMATING DOWNWELLING LONG-WAVE RADIATION, TIGRIS RIVER FROM MOSUL TO BEJEE, IRAQ

Riyad Hassan Al-Anbari | University of Technology
Baghdad, Iraq

Water temperature is one of the most important physical characteristics of aquatic systems. The governing equations of fluid motion and of heat conservation constitute the basis of a mathematical model for water temperature simulation. For the purposes of water temperature modeling, long-wave radiation is specified as one of two types: downwelling radiation is emitted by the atmosphere, upwelling radiation is emitted by the water surface. Mathematical models of temperature for many rivers in the world have been established, but there is not one for the Tigris River in Iraq. This work is an effort to estimate downwelling long-wave radiation from Mosul to Bejee which are near the Tigris River. Daily, weekly and monthly downwelling long-wave radiation with cloudiness were calculated using data from Mosul and Bejee meteorological stations. Correlation coefficients show that monthly averages can be taken to represent the simulation period. Linear regression coefficients of downwelling long-wave radiation from Mosul to Bejee have been established for any time, distance and cloudiness.

INTRODUCTION

Water temperature is one of the most important physical characteristics of aquatic systems. It affects a number of water quality parameters that are of concern for domestic, environmental, industrial, and agricultural applications. Gas solubility decreases and mineral solubility increases with increasing water temperature. Chemical and biological reaction rates increase with increased water temperature. The toxicity of contaminants and the efficacy of water treatment, as well as taste and odor are also affected by water temperature. Further, the evolution, distribution, and ecology of aquatic organisms are fundamentally affected by water temperature. Growth and respiration rates are temperature dependent, and most organisms have distinct temperatures ranges within which they reproduce and compete.

Temperature is also important for some industrial and agricultural supplies. Coordinating temperature management of the different uses of water with environmental needs is a challenge (Michael et al., 2000).

In addition to these more fundamental concerns, in recent years there has been an increasing interest in the potential impact of global warming on the thermal structure of aquatic systems (Pavlakis et al., 2004). Such impacts may have far reaching implications on water resources development, operation, and management in the future.

Models typically include a set of relationships that, either through correlation or through cause and effect functions, aim to yield an increased understanding of a process or processes. To various degrees, models provide representations of complex natural systems (Michael et al., 2000).

The governing equations of fluid motion (flow) and of heat conservation (temperature) constitute the basis of a mathematical model for water temperature simulation (Michael et al., 2000).

Heat transfer at a free surface is generally classified according to classical concepts: radiation, convection, conduction, and evaporation. For numerical modeling of water surface heat fluxes, it is convenient to classify heat transfer in terms of its ability to penetrate through the water surface. Evaporation, conduction, and long wave radiation are all surface heat transfer effects that occur only at the surface of the water. Short-wave radiation is a penetrative effect that distributes its heat through a significant range of the water column (Hodges, 1998).

Radiation emitted by terrestrial objects and the Earth's atmosphere in approximate temperature range 200-300 ^{o}K is termed long-wave radiation (McIntosh, 1972). For the purposes of water temperature modeling, long-wave radiation is specified as one of two types: downwelling radiation (q_{atm}) is emitted by the atmosphere, upwelling radiation (q_b) is emitted by the water surface. Radiation emitted by the earth's atmosphere toward the water surface is positive in sign, and is a strong function of air temperature. Radiation emitted by the water's surface is negative in sign, and is a strong function of water temperature (Michael et al., 2000; Shanahan, 1984).

Mathematical models of temperature for many rivers in the world have been established in order to control environmental requirements. Examples include the Youghiogheny River (Schreiner and Birky, 1997), the Lochsa River (Kent, 2002), and the Chelan River (Payne, 2002). These efforts have been carried out using heat energy budget at water bodies (Hodges, 1998), analysis of current and historical water quality data (Fuhrer et al., 1996), regression models (Neumann et al., 2003), or other related methods.

The Tigris River is one of the two major rivers in Iraq with many activities on its banks (industrial, agricultural, domestic, power-plants). Control of its temperature is very important, and until now no record or monitoring of this property has been conducted.

To apply the energy budget modeling method, long-wave radiation (upwelling, downwelling) must be known, but there are no direct recorded data. This paper is an effort to estimate the downwelling long-wave radiation component of the overall heat budget of the Tigris from Mosul to Bejee, a distance of about 200 Km.

DEFINITIONS

These expressions used later have the following definitions:

Stefan-Boltzmann law: The Stefan-Boltzmann law states that "The total radiation in all directions from an element of a perfect radiator is proportional to the fourth power of its absolute temperature." (McIntosh et al., 1972). Long-wave radiation is typically calculated using the general form of the Stefan-Boltzmann equation,

$$q_{lw} = \varepsilon \sigma T^4 \tag{1}$$

where ε is emissivity, σ is Stefan-Boltzmann constant ($5.67*10^{-8}$ $Wm^{-2}K^{-4}$), and T is temperature in ^oK.

Cloudiness: amount of sky covered by cloud, irrespective of type (McIntosh et al., 1972).

Okta: Unit, equal to area of one eighth of the sky, used in specifying cloud amount (McIntosh et al., 1972), Cloud amount measured as 0, 1/8, 2/8, 3/8, 4/8, 5/8, 6/8, 7/8, 8/8 (Roger et al., 1982)

Polar stereographic projection: used to map all or part of the surface of the earth on a plane, it is widely used in numerical weather prediction (Haltiner and Williams, 1980). According to this projection Cartesian coordinates (x y plane horizontal, **z** vertical) may be introduced on the map as

$$x = \frac{2a\cos\varphi\cos\lambda}{1+\sin\varphi} \quad y = \frac{2a\cos\varphi\sin\lambda}{1+\sin\varphi} \quad z = z \tag{2}$$

where a = Radius of the earth = 6371.229 Km (McIntosh et al., 1972), φ = latitude and λ = longitude.

DOWNWELLING LONG-WAVE RADIATION RELATIONSHIPS

Downwelling long-wave radiation that is applied to the water from the atmosphere is a function of air temperature and air vapor pressure based on the Stefan-Boltzmann law (Michael et al., 2005), but many empirical formulae are available for computing it. We list some here:

A commonly used expression is based on work by Michael et al. (2000):

$$q_{atm} = 0.97\sigma\alpha_0\left(1+0.17C_L\right)T_a^6 \tag{3}$$

where q_{atm} is downwelling long wave radiation ($W\ m^{-2}$), T_a is air temperature (^oK), C_L is fraction of sky covered by clouds, α_0 is a proportionality constant = $0.937*10^{-5}$ and σ is the Stefan-Boltzmann constant.

Hodges (1998) shows that downwelling long wave radiation absorbed by water (Wm^{-2}) is computed by

$$Q_{(absorbed)} = \varepsilon_{air}\sigma\left(1+0.17C_{cloud}^{2}\right)\left(273.2+T_{air\,2}\right)^{4}\left(1-R_{t(lw)}\right) \quad (4)$$

where $C_{(cloud)}$ is the fractional cloud cover, $T_{air\,2}$ is the air temperature (dry bulb in Celsius degrees) measured two meters above the water surface, and R_t is the total reflectivity of the water surface for long wave radiation ($0 = R_{t(lw)} = 1$), non-dimensional. σ is the Stefan-Boltzmann constant.

The formula attributed for the emissivity of the air is:

$$\varepsilon_{air} = C_{\varepsilon}\left(273.2+T_{air\,2}\right)^{2} \quad (5)$$

where C_{ε} is a dimensional empirical coefficient, with a range of values $0.906 \times 10^{-5} < C_{\varepsilon} < 0.99 \times 10^{-5}$.

Michael et al. (2005) state that atmospheric long-wave radiation is a heat flux that is applied to the water from the atmosphere, as a function of air temperature and air vapor pressure, and based on the Stefan-Boltzmann law it can be computed as:.

$$J_{an} = \sigma\left(T_{air}+273\right)^{4}\left(A+0.031\sqrt{e_{air}}\right)\left(1-R_{L}\right) \quad (6)$$

where J_{an} is the atmospheric long-wave radiation (cal cm^{-2} d^{-1}), s is the Stefan-Boltzmann constant, T_{air} is the air temperature (C°), A is the atmospheric attenuation coefficient (A =0.6), e_{air} is the air vapor pressure (mmHg), and R_L is the atmosphere reflection coefficient (0.03). The atmospheric attenuation term ($A+0.031\sqrt{e_{air}}$) and the reflection term (1-R_L) are both generally <1, and therefore have the effect of reducing the influence of the Stefan-Boltzmann heat flux, $\sigma\left(T_{air}+273\right)^{4}$, in the atmospheric long-wave heat flux computation .These two factors combine to compensate for an emissivity value (ε) which would normally be found in the Stefan-Boltzmann law.

The first relationship (Michael et al., 2000) is a commonly used formula (as it has the least requirement for available data) and it has been selected to be used in this paper to calculate the downwelling long-wave radiation from Mosul to Bejee for the Tigris River.

PROCEDURE

As downwelling long-wave radiation is a strong function of air temperature, the meteorological data (daily air temperature) for each day of the year from 1994 to 2000 of the two stations (near the Tigris River) in Mosul (latitude 36° 19' , longitude 43° 9') and Bejee (latitude 34° 54', longitude 43° 32') were provided by the meteorological stations in these locations.

Daily, weekly, and monthly average air temperatures have been calculated over this period of time to get the averages in terms of one year for calculation purposes later.

Assuming different cloudiness (0, 1/8, 2/8, 3/8, 4/8, 5/8, 6/8, 7/8, 8/8) (i.e. 0, 1, 2 ... okta), with the daily, weekly, monthly averages of air temperature for the two stations, the downwelling long-wave radiation has been calculated.

The correlation coefficients between daily with weekly, daily with monthly, and weekly with

monthly of downwelling long-wave radiation for the two stations have been calculated, using the data for air temperature at the fifteenth of each month from daily averages, the beginning of the third week from the weekly averages, finally the monthly averages.

The x and y coordinates for each station have been computed using the Polar stereographic projection, the distance between the two stations is found from the well-known relation between x and y coordinates of the two points.

Assuming linear regression as an approximate relation between magnitudes of downwelling long-wave radiation from Mosul to Bejee, the coefficients of the equations have been found for each cloudiness condition and for any time of the year at any distance from the Mosul station.

In order to show the time of extreme changes of magnitude of downwelling long-wave radiation from Mosul to Bejee the values of the slopes of the linear regressions for all months have been computed.

RESULTS

Figures 1, 2, and 3 show daily, weekly and monthly downwelling long-wave radiation with different fractions of sky covered by clouds respectively using data from the Mosul meteorological station.

Figures 4, 5, and 6 show daily, weekly and monthly downwelling long-wave radiation with different fractions of sky covered by clouds respectively using data from the Bejee meteorological station.

The correlation coefficients of the two stations are shown in Table 1.

The Cartesian coordinates (x,y) in Km, of the two stations are Mosul (4696.551, 4405.996), Bejee (4811.998, 4572.728), and the distance between these two stations is 202 Km.

As there is an excellent correlation between daily, weekly, and monthly averages of downwelling long-wave radiation, the monthly averages has been taken to find the linear regression coefficients. The following relationship was used: $y = ax + b$ where y = downwelling long-wave radiation (W m^{-2}) a = slope, x = distance from Mosul station (Km), and b = intercept.

Table 2 shows linear regression coefficients of downwelling long-wave radiation from Mosul to Bejee.

Figure 7 shows the relation of linear slope with time for downwelling long-wave radiation from Mosul and Bejee

DISCUSSION AND CONCLUSIONS

From the above results the following points can be noted:

From Figures 1 to 6, for each cloudiness and at any time of the year (day, week, and month) the downwelling long-wave radiation of Mosul and Bejee can be determined.

The maximum downwelling long-wave radiation in Mosul and Bejee was at the beginning of the third week of July because of high air temperature at that time of the year.

From Table 1, the very good correlation coefficient (close to 1) allows the use of monthly averages to represent the downwelling long-wave radiation in Mosul and Bejee.

Table 2 represents the mathematical models used for estimation of downwelling long-wave radiation at any time, cloudiness, and distance from Mosul station to Bejee.

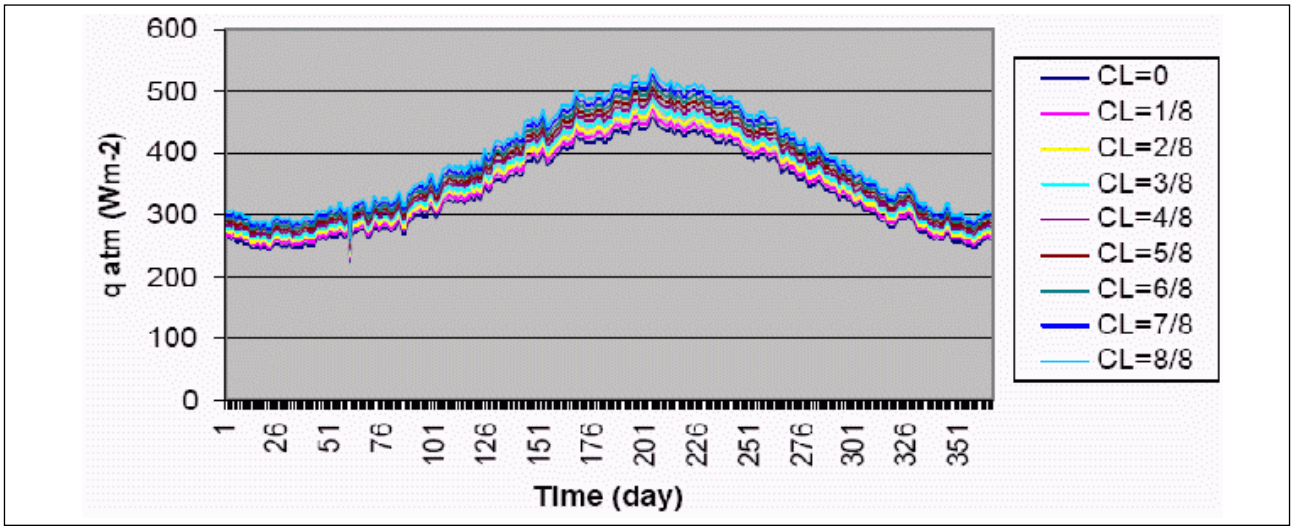

Figure 1. Daily downwelling long wave radiation with different fractions of sky covered by clouds, at Mosul station.

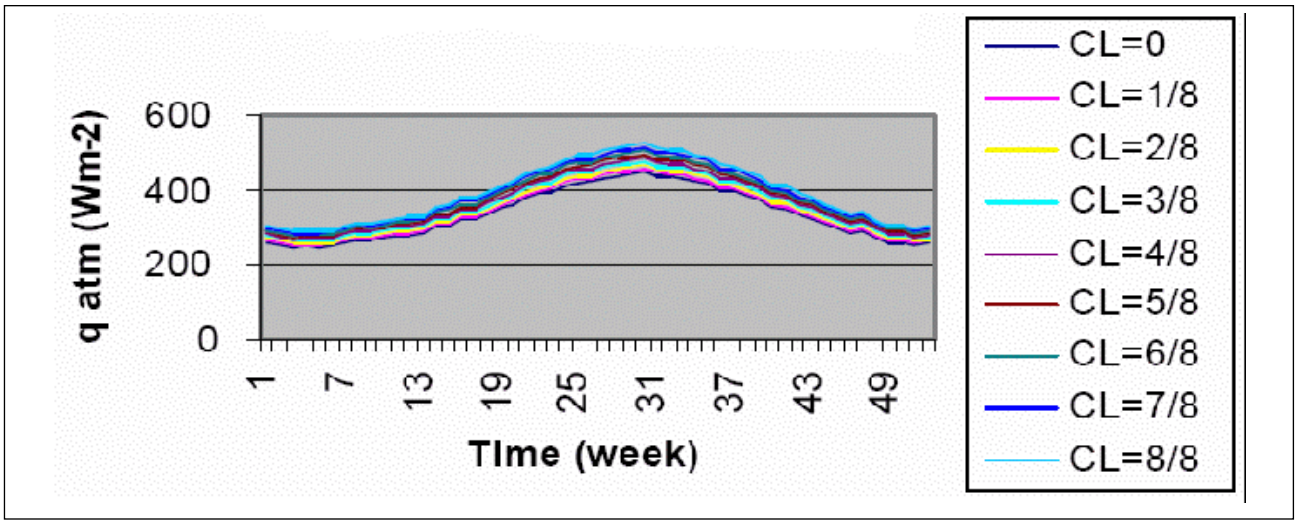

Figure 2. Weekly average downwelling long wave radiation with different fractions of sky covered by clouds, at Mosul station.

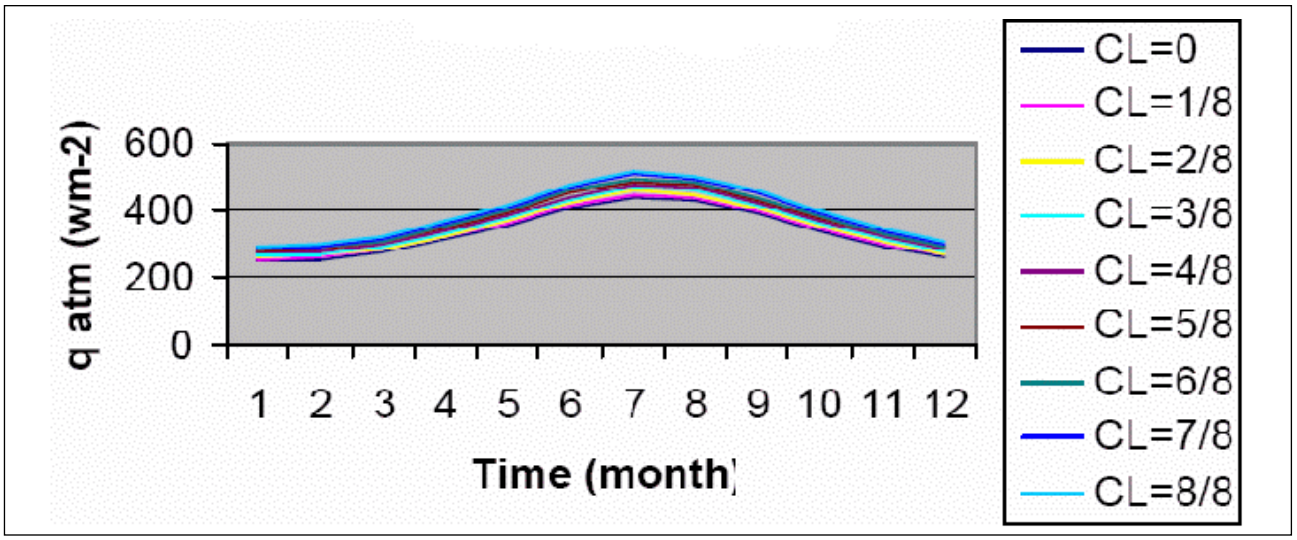

Figure 3. Monthly average downwelling long wave radiation with different fractions of sky covered by clouds, at Mosul station.

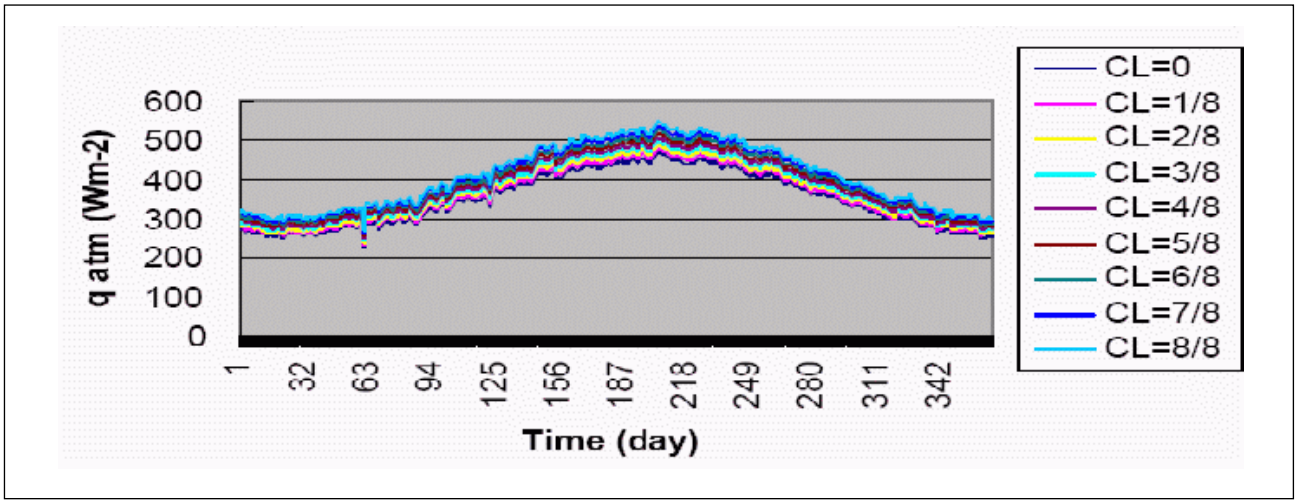

Figure 4. Daily downwelling long wave radiation with different fractions of sky covered by clouds, at Bejee.

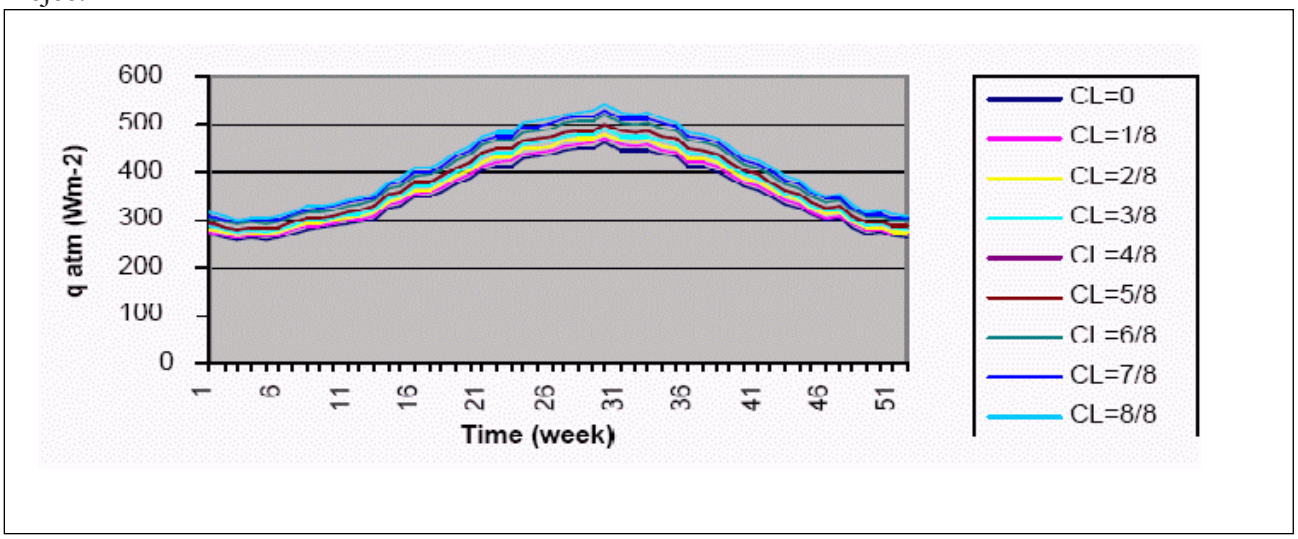

Figure 5. Weekly downwelling long wave radiation with different fractions of sky covered by clouds, at Bejee.

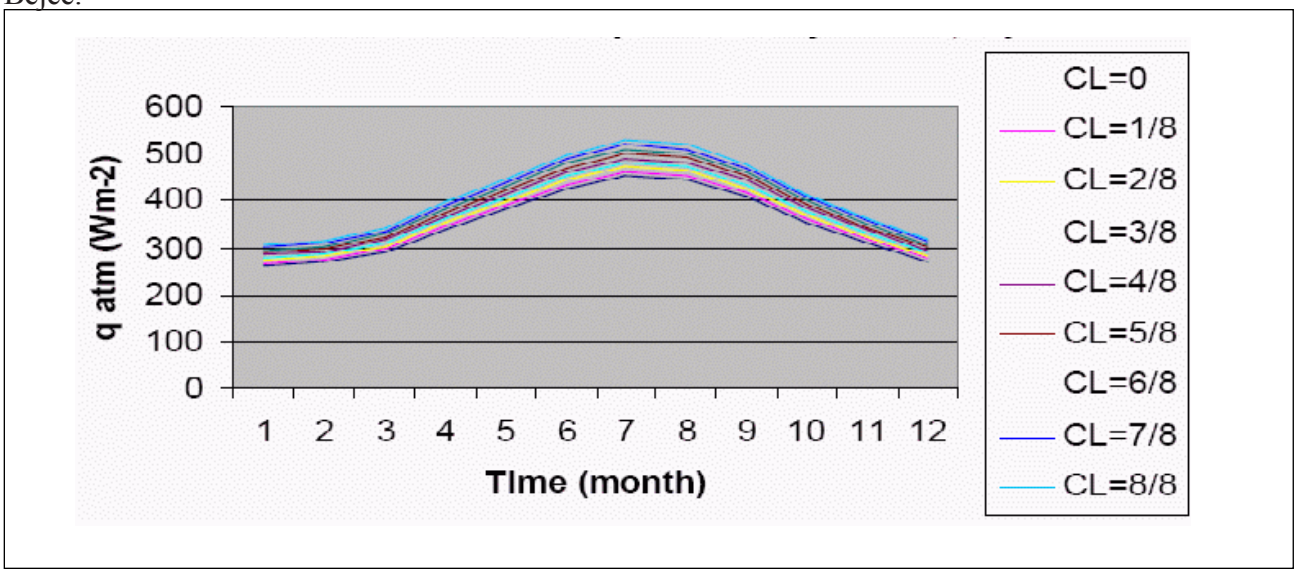

Figure 6. Monthly downwelling long wave radiation with different fractions of sky covered by clouds, at Bejee.

Table 1. Correlation coefficients

Station	Daily & weekly av.	Daily & monthly av.	Weekly & monthly av.	Remarks
Mosul	0.998	0.997	0.996	For all C_L
Bejee	0.998	0.997	0.996	For all C_L

Table 2. Linear regression coefficients of downwelling long-wave radiation from Mosul to Bejee

MONTH	Coefficient	CL=O	CL=1/8	CL=2/8	CL=3/8	CL=4/8	CL=5/8	CL=6/8	CL=7/8	CL=8/8
1.000	b	252.224	257.584	262.944	268.303	273.663	279.023	284.383	289.742	295.102
	a	0.050	0.051	0.052	0.053	0.054	0.055	0.056	0.057	0.058
2.000	b	256.607	262.060	267.512	272.965	278.418	283.871	289.324	294.777	300.230
	a	0.060	0.062	0.063	0.064	0.065	0.067	0.068	0.069	0.071
3.000	b	275.424	281.277	287.129	292.982	298.835	304.688	310.540	316.393	322.246
	a	0.079	0.081	0.082	0.084	0.086	0.087	0.089	0.091	0.092
4.000	b	312.742	319.388	326.033	332.679	339.325	345.971	352.616	359.262	365.908
	a	0.126	0.128	0.131	0.134	0.136	0.139	0.142	0.144	0.147
5.000	b	356.549	364.126	371.702	379.279	386.856	394.432	402.009	409.586	417.162
	a	0.126	0.129	0.132	0.134	0.137	0.140	0.142	0.145	0.148
6.000	b	407.098	415.749	424.400	433.051	441.702	450.352	459.003	467.654	476.305
	a	0.092	0.094	0.095	0.097	0.099	0.101	0.103	0.105	0.107
7.000	b	439.604	448.945	458.287	467.628	476.970	486.312	495.653	504.995	514.336
	a	0.062	0.063	0.065	0.066	0.067	0.069	0.070	0.071	0.073
8.000	b	430.331	439.476	448.620	457.765	466.909	476.054	485.198	494.343	503.488
	a	0.070	0.071	0.072	0.074	0.075	0.077	0.078	0.080	0.081
9.000	b	392.149	400.482	408.815	417.148	425.481	433.814	442.147	450.481	458.814
	a	0.083	0.085	0.086	0.088	0.090	0.092	0.094	0.095	0.097
10.000	b	339.585	346.802	354.018	361.234	368.450	375.666	382.883	390.099	397.315
	a	0.074	0.076	0.077	0.079	0.080	0.082	0.084	0.085	0.087
11.000	b	296.154	302.447	308.740	315.034	321.327	327.620	333.913	340.207	346.500
	a	0.067	0.068	0.070	0.071	0.073	0.074	0.076	0.077	0.078
12.000	b	260.774	266.316	271.857	277.399	282.940	288.482	294.023	299.565	305.106
	a	0.054	0.055	0.056	0.057	0.058	0.060	0.061	0.062	0.063

*y = ax +b, where y = downwelling long-wave radiation (W m^{-2}), a = slope, x = distance from Mosul station (Km), b = intercept.

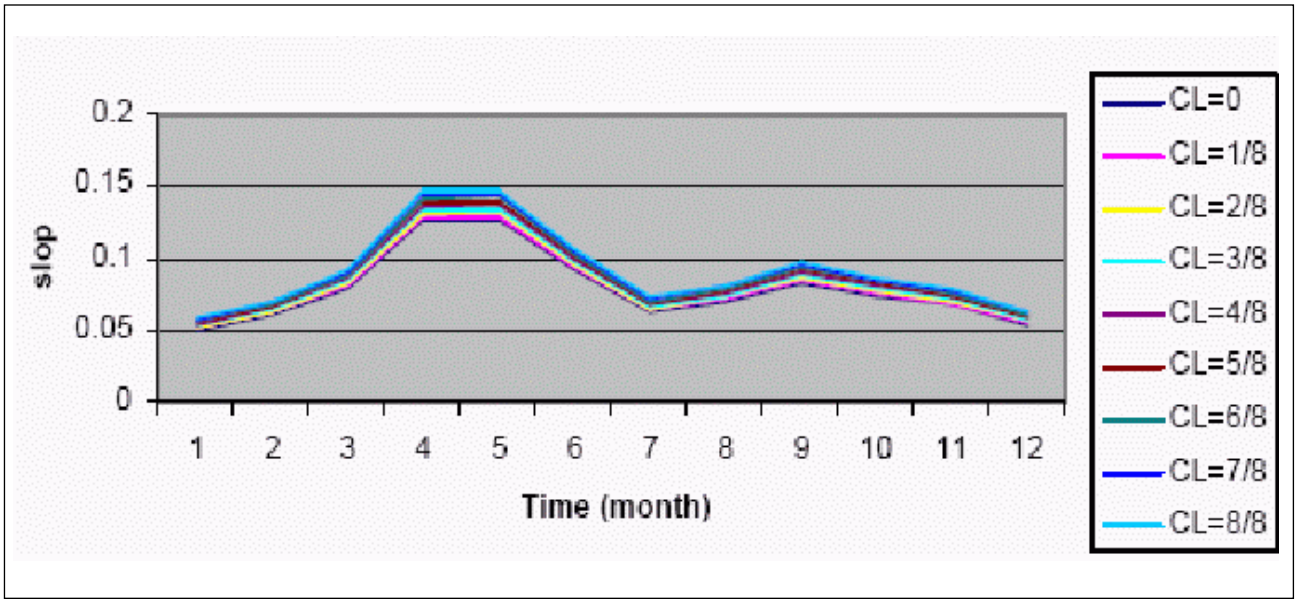

Figure 7. Relation of linear slope with time for downwelling long-wave radiation from Mosul to Bejee.

From Figure 7 it is clear that there is extreme change (great difference in magnitude) in downwelling long-wave radiation between Mosul and Bejee in April and May, and it reaches the minimum change (low difference in magnitude) during January, July and December. For March and September there is a mild change.

ACKNOWLEDGMENTS

The author would like to acknowledge the reviewers Dr. Adnan Al-Samawi, Ph.D., Environmental Engineering, University of Technology, Baghdad, Iraq, and Dr. Karim K. Al-Jumaily, Ph.D. Hydraulic and Water Engineering, University of Technology, Baghdad, Iraq, for their help and reviewing this paper.

The author would like also to acknowledge Dr. Tariq A. Mahmood, University of Mosul, Iraq, and give a special acknowledgement to Miss Wafa Fawzi Yousif, M.Sc. in Civil Engineering, Technical Institute, Mosul, deceased in December, 2005. She was very active, honest, and was a hard worker. She helped me in greatly in data collection and calculations. My condolences to her family and colleagues.

REFERENCES

Hodges, B. 1998. Heat budget and thermodynamics at a free surface: Some theory and numerical implementation. Center for Water Research. The University of Western Australia. June 9, 1998

Fuhrer, G.J., D.Q. Tanner, J.L. Morace, S.W. McKenzie, and K.A. Skach. 1996. Water Quality of the Lower Columbia River Basin: Analysis of Current and Historical Water-Quality Data through 1994. U.S. Geological Survey, Water-Resources Investigations Report 95–4294, Portland, Oregon.

Haltiner, G.J., and R.T. Williams. 1980. Numerical prediction and dynamic meteorology. John Wiley & Sons.

Kent, J. 2002. Lochsa river temperature model. HDR Engineering, Inc., for Idaho department of environmental quality.

McIntosh, D.H. 1972. Meteorological glossary. Her Majesty's Stationery office, London.

Michael, N., K. Strzepek, and S.C. Chapra. 2005. Modeling the potential effects of climate change on water temperature downstream of a shallow reservoir, lower Madison river, MT. Climatic Change 68: 331–353.

Michael, L., C. Deas, and C.L. Lowney. 2000. Water temperature modeling review central valley. Bay Delta Modeling Forum.

Neumann, D.W., B. Rajagopalan, and E.A.Zagona. 2003. Regression Model for Daily Maximum Stream Temperature. Journal of Environmental Engineering, ASCE. July 2003:667.

Pavlakis, K.J., D. Hatzidimitriou, C. Matsoukas, E. Drakakis, N. Hatzianastassiou, and I. Vardavas. 2004. Ten-year global distribution of downwelling longwave radiation. Atmos. Chem. Phys., 4, 127–142.

Payne, T.R. 2002. Chelan river stream network temperature model, Lake Chelan hydroelectric project, FERC project No. 637. Public utility district No. 1 of Chelan county, Washington.

Roger, G., R. Barry, and R.J. Chorley. 1982. Atmosphere, weather and climate. Methuen, London and New York.

Schreiner, S.P., and G.D. Birky. 1997. A temperature simulation model of the Youghiogheny river from Deep creek station to Sang Run. Maryland power plant research program.

Shanahan, P. 1984. Water temperature modeling: A practical guide. EPA, proceedings of storm water and water quality model users. Group Meeting. April 12-13, 1984.

ADDRESS FOR CORRESPONDENCE
Riyad Hassan Al-Anbari
University of Technology
Baghdad, Iraq

Email: riyadhassan2003@yahoo.com